Inversion of GPS measurements for a layer of negative dislocation distribution in north China

J. C. Wu,[1] H. W. Tang, and Y. Q. Chen
Department of Land Surveying and Geo-Informatics, Hong Kong Polytechnic University, Hong Kong, China

Y. X. Li
First Crustal Deformation Monitoring Center, China Seismological Bureau, Tianjin, China

Received 27 August 2002; revised 2 July 2003; accepted 22 July 2003; published 17 October 2003.

[1] In north China, most earthquakes occur at depths of 10–25 km and are considered to be the direct result of deformation or rupture of the brittle upper crustal layer. To describe this mechanism, a planar horizontal negative dislocation plane is used to represent the force of action of the lower crustal layer on an overlying brittle upper crust layer. An area around Beijing in north China has been chosen for applying this negative dislocation layer assumption. A GPS network (Capital Circle GPS Network, CCGN), has been set up for monitoring crust deformations since 1992. In this paper, observations from 1992, 1995, and 1996 GPS surveying campaigns were used to determine model parameters of a negative dislocation layer. Using a Bayesian inversion procedure, more than 95% of data residuals are found to be <2 mm/yr, indicating that the negative dislocation layer model can fit GPS data well. The inversion results show that the local tectonic movement is -2 ± 1 mm/yr in the north and 7 ± 1 mm/yr in the east, and the high negative dislocation rates occur mainly in the south part of the north Taihang mountain zone with a magnitude of $\sim 4 \pm 1$ mm/yr, and the east part of the Yan mountain zone with a magnitude of $\sim 3 \pm 1$ mm/yr. By applying this negative dislocation layer model, the continuous GPS surveying data can be inverted to determine the negative dislocation rate distributions in the middle or upper seismogenic crust layer, so as to predict the locations of potential earthquake sources. *INDEX TERMS:* 1208 Geodesy and Gravity: Crustal movements—intraplate (8110); 1243 Geodesy and Gravity: Space geodetic surveys; 7209 Seismology: Earthquake dynamics and mechanics; 8107 Tectonophysics: Continental neotectonics; *KEYWORDS:* GPS, inversion, layer negative dislocation model, north China

Citation: Wu, J. C., H. W. Tang, Y. Q. Chen, and Y. X. Li, Inversion of GPS measurements for a layer of negative dislocation distribution in north China, *J. Geophys. Res.*, *108*(B10), 2481, doi:10.1029/2002JB002171, 2003.

1. Introduction

[2] China is located in the southeast front of the Eurasia Plate (Figure 1). Its tectonic movements are mainly controlled by the interplate collision between the India Plate and Eurasia Plate at the southwest boundary and the subduction of the west Pacific Plate and Philippine Plate under the Eurasia Plate at the southeast boundary [*Ye et al.*, 1987; *Ma*, 1989]. The India-Eurasia plate collision causes the Tibetan Plateau to rise and move toward the northeast [*Molnar and Tapponnier*, 1975; *Peltzer et al.*, 1989; *Royden et al.*, 1997]. The tectonic movements of the Tibetan Plateau further push north China along the southwest boundary of the Ordos block in the east direction (Figure 1). The space geodetic surveys since 1990 show that the north China block moves at ~5–11 mm/yr in the southeast direction relative to the Eurasia Plate [*Shen et al.*, 2000; *Wang et al.*, 2001]. This is in accord with the local tectonic movements noted from geological investigations [*Ma*, 1989; *Northrup et al.*, 1995]. Local tectonic movements are controlled by surrounding plate movements and interior mantle convections, and they are usually assumed to be constant both in their direction and magnitude in hundreds of years [*Matsu'ura et al.*, 1986; *Wu*, 1999]. *Li and Rice* [1987] and *Roy and Royden* [2000] proposed a base traction model to describe the crust deformations in plate boundaries. A constant shear flow zone is supposed to exist in depth under the plate boundary. Their models have successfully explained data from geodetic and geological investigation at strike-slip plate boundaries. However, for an intraplate area, such as north China, neither significant active strike-slip faults nor a shear flow zone in depth exist as in the transform plate boundary. Instead, a uniform lower crust flow is assumed to exist at depth, and the overlying upper crust is believed to move and deform as a whole unit. Their models will therefore not be suitable to this case. On the other hand, a layer with horizontal stress accumulation

[1]Now at Department of Surveying, Tongji University, Shanghai, China.

0148-0227/03/2002JB002171$09.00

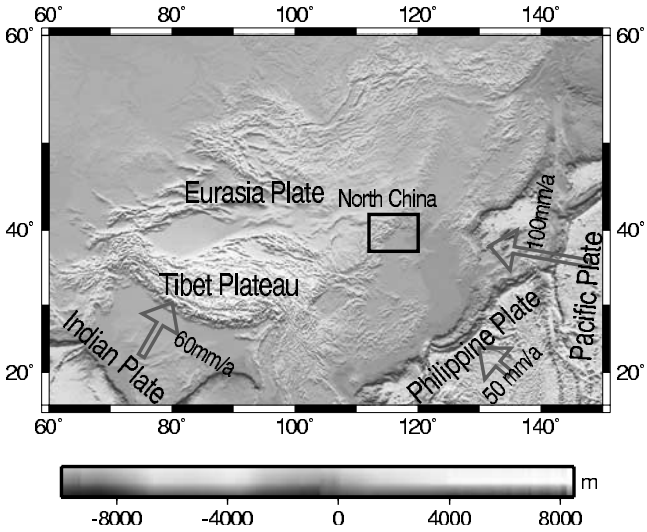

Figure 1. Tectonic setting of China. Rectangular box is the location of North China Basin. The background topographical image is drawn based on the data file, top.8.2.img, which is distributed by GMT software (same of the background images in the Figures 3–6).

really exists in depth in the North China Basin [*Zeng et al.*, 1995]. This evidence supports our uniform lower crust flow assumption. In this paper, we propose a horizontal negative dislocation layer model to describe the crustal deformation in the intraplate area such as north China.

[3] Because of anisotropic rock strength and geological structures in the upper crust, the uniform local tectonic movement imposed in the lower crust can lead to impeded patches between the lower and upper crustal layers. The observed crustal deformations at the surface are then the superposition of steady local tectonic movements and those caused by impeded patches on the lower moving crustal layer.

[4] In the following, a horizontal layer of negative dislocation distributions is first proposed to represent the impeded patches or stress accumulation in depth. Then the velocities of the CCGN stations obtained by GPS surveys are used to determine the negative dislocation distributions at a specific depth through a Bayesian inverse procedure. The inversion results show that the layer dislocation model can fit GPS observations very well and the high negative dislocation rates are located in the south part of the north Taihang mountain zone and the east part of Yan mountain zone.

2. Methodology

[5] In the Earth's crust, tectonic movements originate from the movement of the deep bottom layer and pass to the upper layer [*Li and Rice*, 1987; *Roy and Royden*, 2000]. *Li and Rice* [1987] proposed the base traction model which takes into account the coupling between the viscously relaxing asthenosphere-like lower crustal layer and the overlying elastic middle and upper crusts. They think the asthenosphere-like lower crustal layer moves at a stable velocity and drives the overlying upper crust. *Roy and Royden* [2000] proposed a rheological model to relate surface deformations to the stress transmission in the crust. However, their models are based on the transform plate boundary zone and are difficult to apply to an intraplate area. For an intraplate area, such as north China, we assume that crustal deformation is mainly caused by the coupling between the uniform lower crust flow and the overlying brittle upper crust. There exist no shear flow zones at depth as in the transform boundary. The upper crustal layer more likely deforms as a whole unit. On the other hand, because of anisotropic rock strength and geological structures in the passive upper crust layer, the induced movements and deformation in the upper crust will be heterogeneous. Some impeded patches will be formed at depth (Figure 2). These patches will cause deformation in the overlying crustal layer and further cause faulting or earthquakes around their boundaries in the upper crust. We further assume that the crustal deformation caused by these impeded patches can be represented by a negative dislocation model [*Matsu'ura et al.*, 1986; *Wu*, 1999].

[6] So, the site velocities observed are equal to the sum of the constant local tectonic movement and the deformation rate caused by a number of impeded patches in depth (Figure 2). Furthermore, a horizontal plane with variable negative dislocation distributions will be used to describe the crustal deformations of all the impeded patches in depth. So, we get:

$$y = V + f_{\Sigma} + \varepsilon, \tag{1}$$

where y is the vector of observed velocities of GPS stations, ε is the random observation error vector, V is the velocity vector of the constant local tectonic movement, and f_{Σ} is the deformation rate vector of functions by the horizontal planar negative dislocation layer Σ. Obviously, this is a first-order approximation of the real crust deformation because we have omitted the possible effects caused by induced faulting in the upper crust layer. We believe that these effects are small during our surveying periods. According to the dislocation solutions in semi-infinite isotropic elastic medium by *Okada* [1985], f_{Σ} is a function of the

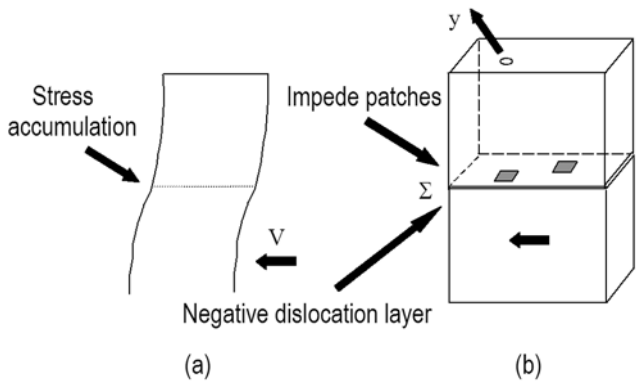

Figure 2. Negative dislocation layer model. (a) Vertical section of shear deformation about impeded patches. (b) Lower layer which drives the upper layer. V is the velocity of the constant local tectonic movement, y is ground surface site movement observed, and Σ is the supposed negative dislocation layer in depth.

geometrical parameters of a dislocation plane such as the length, width, dip angle, and the dislocation values distributed on Σ. If the geometrical parameters are fixed, f_Σ will be a linear function of dislocation values. In our model, we divide the planar horizontal negative dislocation plane in depth into $N \times M$ grids with grid step of ΔS_N and ΔS_M in the north and east, respectively, and suppose that the geometrical parameters of the negative dislocation layer are known and fixed; then the observation (1) can be written as

$$y = V + \sum_i^N \sum_j^M f_\Sigma(U_{1ij}, U_{2ij}) + \varepsilon, \tag{2}$$

where U_{1ij}, U_{2ij} are the strike and dip (i.e., east and north) components of the dislocation rate of the ijth grid on the dislocation plane Σ (for simplicity, we have omitted the tensile dislocation components in this research work). The least squares method can be used for determining the dislocation distributions if the number of observations is greater than the number of total unknown parameters based on equation (2). However, to get a detailed distribution of negative dislocation distributions, the grid step should be small, e.g., $30'$ or $10'$; then the unknown parameters will be increased dramatically and will be larger than the number of observations. Equation (2) will be underdetermined. In this case, a Bayesian inverse procedure [*Matsu'ura et al.*, 1986; *Wu*, 1999] will be used to determine the unknown parameters by supplying additional a priori information of unknown parameters. In our inversion work, the a priori information for the unknown dislocation values will be supposed to obey a normal distribution with expectation zero and a known covariance, Σ_x, that is,

$$x = x_0 + e, \tag{3}$$

where x is the unknown parameter vector of the negative dislocation components of all grids and the local tectonic movement velocity, i.e.,

$$x = [U_{111}, U_{211}, ..., U_{1MN}, U_{2MN}, V_N, V_E]^T, \tag{4}$$

V_N, V_E are north and east components of the local tectonic velocity V, x_0 is the a priori value, e is the corresponding random error vector, and

$$e \sim N(0, \Sigma_x). \tag{5}$$

On the basis of equation (4), equation (2) can be rewritten as

$$y = f(x) + \varepsilon, \tag{6}$$

where

$$f(x) = V + \sum_i^N \sum_j^M f_\Sigma(U_{1ij}, U_{2ij}). \tag{7}$$

Similarly, we suppose that the observational random errors in equation (6) follow the normal distribution, i.e.,

$$\varepsilon \sim N(0, \Sigma_y), \tag{8}$$

where Σ_y is a covariance matrix of observation data, which can be filled with the known variances of observed GPS velocities.

[7] On the basis of the Bayesian inversion method, an iteration procedure for solving x is listed as follows [*Matsu'ura et al.*, 1986]:

$$x_{k+1} = x_k + M_k^{-1} r_k, \tag{9}$$

where

$$M_k = A_k^T \Sigma_y^{-1} A_k + \Sigma_x^{-1}, \tag{10}$$

$$r_k = A_k^T \Sigma_y^{-1} [y - f(x_k)] + \Sigma_x^{-1}(x_0 - x) \tag{11}$$

the subscript k indicates the iteration times ($k = 0, 1, 2, \ldots$), and the elements of the matrix A_k are calculated by

$$A_{ij} = \left[\frac{\partial f_i}{\partial x_j}\right]_{x=x_k}, \tag{12}$$

where b_k is a step factor, $0 < b_k \leq 1$; x_0 is the start value vector of x, i.e., a priori value vector of model parameters.

[8] According to the Bayesian inversion theorem, when the solution of model parameters with maximum a posteriori probability is obtained, then equation (11) should be equal to zero [*Wu*, 1999]. So a small positive value γ is assigned as the threshold to determine the end of the iteration. The solution can be defined as

$$\hat{x} = x_{k+1}, \| r_k \| < \gamma. \tag{13}$$

Accordingly, the accuracy of the solution can be expressed by the approximate covariance matrix [*Jackson and Matsu'ura*, 1985]:

$$C_{k+1} = \left(A_{k+1}^T \Sigma_y^{-1} A_{k+1} + \Sigma_x^{-1}\right)^{-1}, \tag{14}$$

and data residuals can be calculated by

$$V = f(x_{k+1}) - y. \tag{15}$$

3. GPS Data and Inversion Results

[9] The CCGN was set up in 1992 with the aim of monitoring crustal deformation around the Beijing area. The First Crustal Deformation Monitoring Center (FCDMC) of the China Seismological Bureau is responsible for the GPS surveying of CCGN. In 1992, 1995, and 1996, three GPS surveying campaigns were conducted. Table 1 shows the total number of GPS sites, observation sessions at each site, and GPS receivers used in each GPS campaign.

[10] *Shen et al.* [2000] processed the GPS surveying data using the GAMIT and QOCA software in a four-step approach. About 16 IGS stations were included in the data processing to ensure a homogenous solution. Parameters of the GPS antenna phase center of each GPS receiver were introduced in data processing to obtain accurate results.

Table 1. The 1992, 1995, and 1996 GPS Surveying Campaigns of CCGN

GPS Campaign	Number of Sessions	Time Period	Number of sites	Instrumentation
1992	3	22	63	Ashtech L-XII, 5 sets
1995	3	22	90	Ashtech Z-XII, 7 sets
1996	4	24	90	Ashtech Z-XII, 8 sets

The velocity solutions of GPS sites are constrained to the NNR (No-Net-Rotation) NUVEL-1A model [*DeMets et al.*, 1990, 1994], and accurate to ~2 mm/yr. The velocities obtained show that the north China region is moving at ~5–11 mm/yr southeastward relative to the stable Eurasia Plate. In this paper we use the velocities of GPS sites published by *Shen et al.* [2000]. Figure 3 shows the residual GPS station velocities relative to the NNR-NUVEL-1A model in our research area. These residual velocities represent the recent local tectonic movements and crustal deformations and can be inverted to determine both the local horizontal tectonic velocities and the negative dislocation distributions on a planar horizontal layer in depth.

[11] In view of the limitation of the GPS data coverage of CCGN, we choose the rectangular area (dashed box in Figure 3), north latitude from 36° to 42° and east longitude from 112° to 120°, to determine its planar negative dislocation distributions in depth. On the basis of the statistics on the depths of historical earthquakes in our research area (Figure 4), we set the depth of the planar horizontal negative dislocation plane at 15 km. The grid size of the dislocation plane was set at 30′ both in the east and north directions. The a priori and a posteriori values of model parameters are listed in Table 2. Also, the negative dislocation distributions obtained are displayed in Figure 5. The distributions of data residuals of each GPS site velocity after inversion are drawn in Figure 6.

4. Discussion and Conclusion

4.1. Uniform Lower Crustal Layer Flow in North China and Implementation of Negative Dislocation Layer

[12] According to *Zeng et al.* [1995] the stress field in the North China Basin is a kind of normal faulting regime in the upper crust of less than 8 km, i.e., $\sigma_z > \sigma_x > \sigma_y$ (where σ_x, σ_y are horizontal major stress components and σ_z is the vertical stress component), but in the middle or lower crust (12–20 km), the focal mechanism of earthquakes shows a stress field of a strike slip faulting, i.e., $\sigma_x > \sigma_z > \sigma_y$, which means that the horizontal stresses are increased greatly in the middle or lower crust layer. In addition, the focal mechanisms of both the 1976 Tangshan earthquake (M = 7.8) and

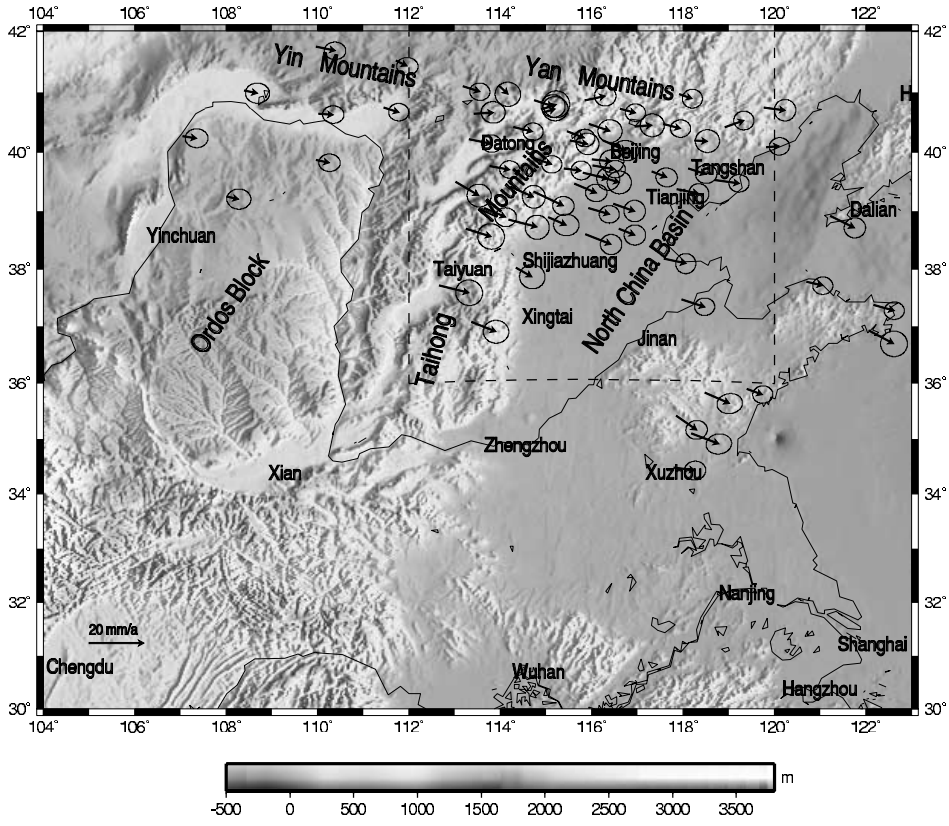

Figure 3. GPS sites residual velocities in north China (based on the work by *Shen et al.* [2000]). Solid arrows are site residual velocities with respect to stable Eurasia Plate based on NNR-NUVEL-1A. Each arrow originates at the location of the station and points to its motion direction. The error ellipses represent 95% confidence. The dashed box is our research area and where the negative dislocation distributions in depth are to be determined.

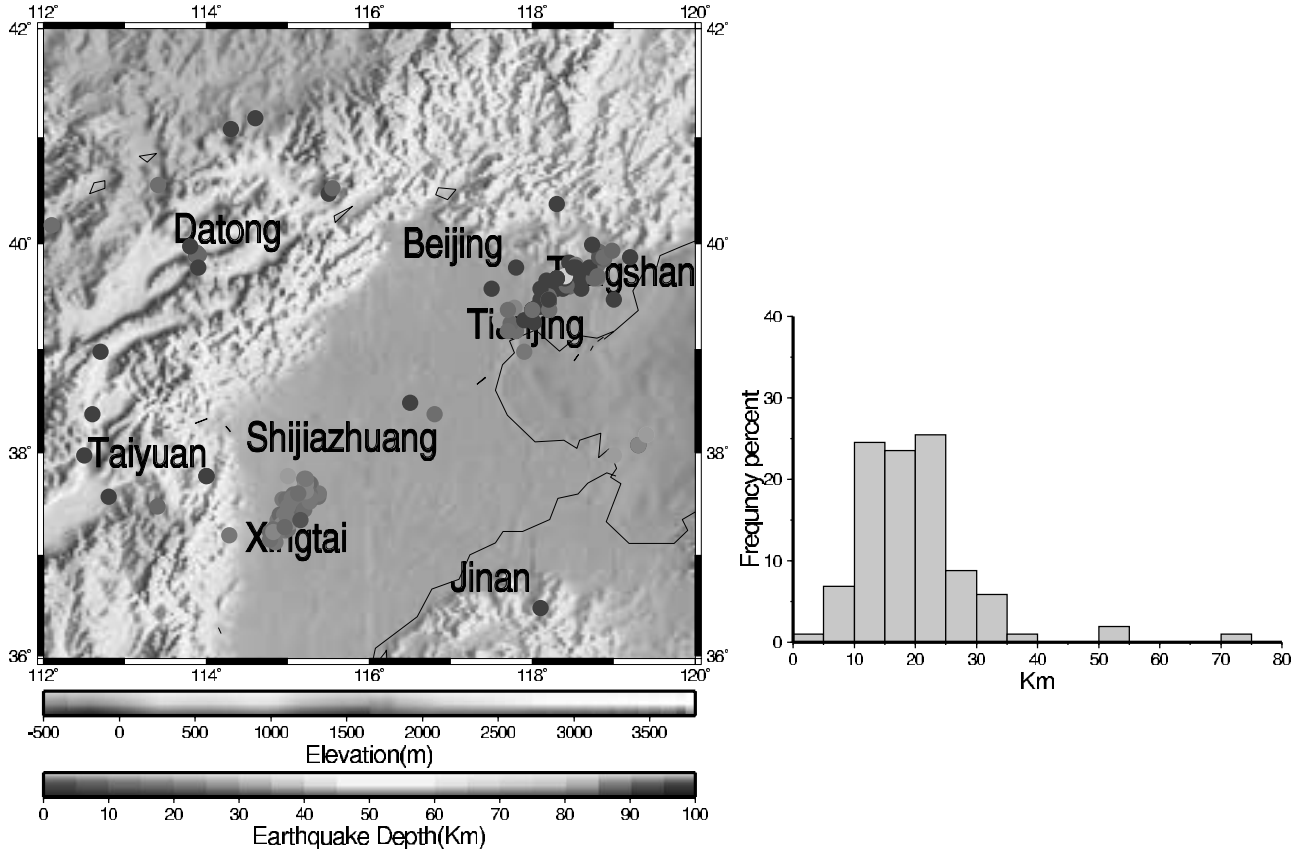

Figure 4. Historical earthquake distribution and frequency based on their epicenter depths in the research area. (The earthquake catalog used is from 1930 to 2001 with magnitude greater than 4.5, which is supplied by W. Z. Wang of the China Seismological Bureau, and some records in the catalog without depth values are assumed at depths from ISC website http://www.isc.ac.uk/.) The centers of shaded circles are the locations of earthquakes.

1966 Xingtai earthquake ($M = 7.2$) are strike-slip faults ($\sigma_x > \sigma_z > \sigma_y$) [*Zeng et al.*, 1995]. Both of these two large earthquakes are located in our research area. We believe that the increase in the horizontal stress in the lower or middle crust layer is induced by a steady flow of a thick layer of lower crust or even upper mantle. This lower crust steady flow represents the local neotectonic movements. It can be described by reference to a uniform lower crust layer flow in deep depth. This lower crust layer flow drives the overlying upper brittle crust layer to move and deform, even though the mechanism driving the lower crust flow is not clear at this moment.

[13] On the other hand, the depths of most significant earthquakes in north China are 10–25 km (Figure 4). For example, the depth of the Xingtai earthquake is 15–20 km, and the depth of Tangshan earthquake is ~10 km. So a negative dislocation plane at 10–20 km will be reasonable to approximate the crust deformation caused by stress accumulations or impeded patches in depth. In our inversion work, we have chosen the planar negative dislocation plane in depths of 8, 10, 15, 25, and 30 km individually and the grid size at 30′ both in the north and east. The distribution patterns of negative dislocation rates obtained are similar. The magnitude of negative dislocation rates increases with the depth of the planar negative dislocation plane. The sum of residual squares also increases with the depth of the planar negative dislocation plane. However, when the depth of the planar negative dislocation plane is 15 km, the data residual distribution approximates well to a normal distribution and the 95% residuals are less than 2 mm/yr (Figure 6). In addition, for considering the effects of grid size, we have chosen a grid size of 18′ and a depth of 15 km; the sum of data residual squares increased about twice of the same depth and with grid size of 30′, which implies that our observations are too sparse to allow us to find a more dense distribution of negative dislocation rates in depth. In the following, we only show and discuss the inversion results at a depth of 15 km and a grid size of 30′.

4.2. Inversion Results and the Uncertainties

[14] As mentioned in section 3, the dashed line area in Figure 3 is chosen to determine the planar negative

Table 2. A Priori and A Posteriori Values of Model Parameters

	Grid Negative Dislocation, m/yr		Local Tectonic Movement, m/yr	
	U1	U2	V_E	V_N
A Priori	0 ± 0.005	0 ± 0.005	0.011 ± 0.002	−0.005 ± 0.002
A Posteriori	Figure 5	Figure 5	0.007 ± 0.001	−0.002 ± 0.001

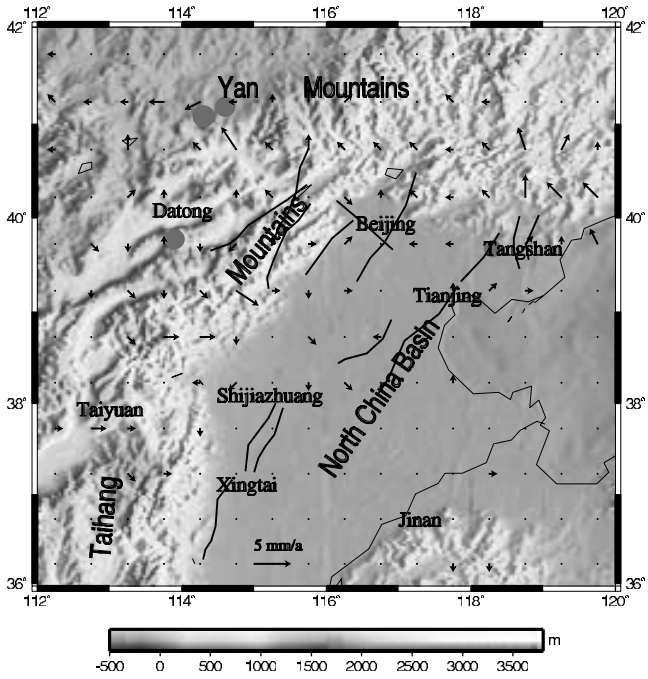

Figure 5. Negative dislocation rate distributions at a depth 15 km. The solid arrows originate at the center of each grid and point to their vector direction. The grid size is 30′. Centers of shaded circles are epicenters of earthquakes with magnitude greater than 4.5 that occurred after 1996. The bold lines are trace of Quaternary active faults.

dislocation rate distributions in depth. We only choose the GPS stations near this specific area for inversion calculations. Sixty GPS station velocities are used. The grid size of the negative dislocation plane is 30′, so there are in total 192 grids for determining their negative dislocation rates. Because we fixed the geometric parameters of the dislocation plane (each grid), the inversion problem here is linear, but it is underdetermined. The number of unknown parameters (386) is greater than the number of observations (120). The a priori information of the unknown parameters must be given in accordance with the Bayesian inversion procedures for obtaining unique solutions [*Matsu'ura et al.*, 1986].

[15] We set the a priori negative dislocation rates of all grids at 0 and with a standard deviation of 5 mm/yr (Table 2). This assumes that the whole upper crust layer is moving at the same rate as the lower crust layer, and there are initially no impeded patches between two layers. The uncertainty of ±5 mm/yr is assigned for considering the possible order of magnitude of velocities at depth. Actually, we have assigned 3 mm/yr as the standard deviation of the a priori negative dislocation rates; the inversion results obtained are almost the same. The a priori values of the local tectonic movements are set at -5 ± 2 mm/yr in the north and 11 ± 2 mm/yr in the east (Table 2). This is the largest velocity of GPS stations observed. To consider the effects of initial values of tectonic movements, we have set a priori values of the local tectonic movements to be 0 ± 2 mm/yr both for the north and east components; the results obtained are almost the same.

[16] From Figure 6, we can see that more than 95% of data residuals between model predictions and observations are smaller than 2 mm/yr, and none are greater than 3 mm/yr, which is comparable to the accuracy of the observations. The local tectonic movement velocities obtained are -2 ± 1 mm/yr in the north components and 7 ± 1 mm/yr in the east components (Table 2). This is a little larger than the geological investigations, 4 mm/yr in the east [*Ma*, 1989].

4.3. Negative Dislocation Rate Distributions and Potential Earthquake Sources

[17] The negative dislocation rate distributions obtained are significant mainly in the south part of the north Taihang mountain zone and the east part of the Yan mountain zone (Figure 5), where the boundary lies between the North China Basin and the east Ordos block and Yan mountain areas, and where the upper crust layer displays obvious transverse heterogeneity in geological structures.

[18] The negative dislocation rates of the south part of the north Taihang mountain zone obtained are different from that of the east part of the Yan mountain zone in their directions. At the south part of the north Taihang mountain zone the negative dislocation rates mainly point toward the southeast, close to the direction of the local tectonic movement, and the largest magnitude of the negative dislocation rate is $\sim 4 \pm 1$ mm/yr. However, at the east part of the Yan mountain zone, the negative dislocation rates mainly point toward the north or northwest, and the magnitude of the negative dislocation rate is $\sim 3 \pm 1$ mm/yr. Because the negative dislocation rate is opposite to the real relative movements [*Matsu'ura et al.*, 1986; *Wu*, 1999], the south part of the north Taihang mountain zone shows a slowdown of the upper crustal layer. That means some impeded patches exist in the depth. The east part of the Yan mountain zone shows that the negative dislocation rates are almost perpendicular or opposite to the obtained local tectonic movement direction. This conflicts somewhat with our proposed model; there must be some local effects not accounted for in our model in the east part of the Yan mountain zone.

[19] In an intraplate area, such as north China, we believe that faults rupture in the brittle upper crust, not between layers. Because the significant negative dislocation area corresponds to significant impeded patches, its boundary in the upper crust should be the potential location of ruptures and earthquakes. Fortunately, no earthquakes with magnitude greater than 4.5 occurred during 1992–1996 in our research area. After 1996, however, some significant earthquakes occurred. We have drawn the locations of earthquakes with magnitude greater than 4.5 after 1996 in Figure 5. Their locations seem to support our boundary rupture assertion above. We also draw Quaternary active faults [*Ma*, 1989] in Figure 5. Across the fault trace, the direction of the negative dislocation rate changes significantly. This also supports our assertion that ruptures occurred at the boundary of impeded patches in depth.

4.4. Limitations and Improvements

[20] The time span of our GPS data used is ~4 years (1992–1996). This is relatively short at the scale of local tectonic processes. The GPS velocities obtained are easily affected by some intermittent non-tectonic events, such as

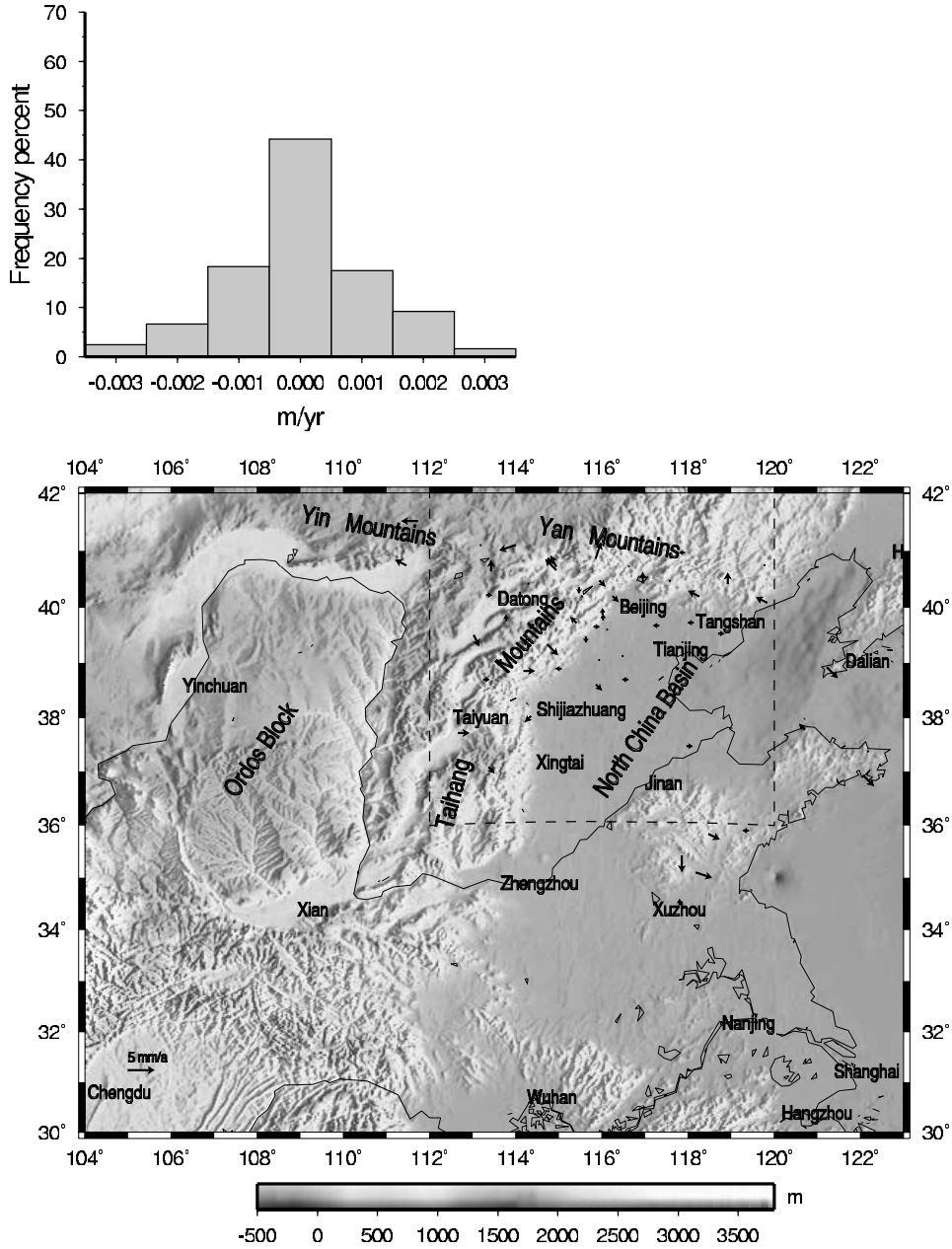

Figure 6. Data residual distributions. (top) Histogram based on the magnitude of data residuals and (bottom) distribution of data residual vectors.

changes in the under groundwater table in short time periods, creeps of some existing shallow fault and so on. In addition, the data are relatively sparse compared to our 30′ grid size density or even higher-density grid size used in outlining the boundary of impeded patches. These shortcomings limit our inversion results, making this something of an initial stage in an ongoing investigation. However, with the continued monitoring of the GPS surveys and increases in the density of the GPS sites (and perhaps the inclusion of other crust deformation data, such as spirit leveling, strains, tilts, and even INSAR observations) and the consideration of intermittent surface movements and active fault movements at surface, the proposed methodology in this paper shows a possible way to determine the locations and strength of impeded patches, so as to recognize the potential earthquake sources in the intraplate area.

[21] **Acknowledgments.** The work described in this paper has been supported by a grant from the Research Grant Council of the Hong Kong Special Administrative Region, China (Project PolyU5073/00E).

References

DeMets, C., R. G. Gordon, S. Steinand, and D. F. Argus, Current plate motions, *Geophys. J. Int.*, *101*, 425–478, 1990.

DeMets, C., R. G. Gordon, D. F. Argus, and S. Stein, Effect of recent revisions to the geomagnetic reversal time scale on estimates of current plate motions, *Geophys. Res. Lett.*, *21*, 2191–2194, 1994.

Jackson, D. D., and M. Matsu'ura, A Bayesian approach to nonlinear inversion, *J. Geophys. Res.*, *90*, 581–591, 1985.

Li, V. C., and J. R. Rice, Crustal deformation in great California earthquake cycles, *J. Geophys. Res.*, *92*, 11,533–11,551, 1987.

Ma, X., (Ed.), *Lithospheric Dynamics Atlas of China*, China Cartogr., Beijing, 1989.

Matsu'ura, M., D. D. Jackson, and A. Cheng, Dislocation model for aseismic crustal deformation, at Hollister, California, *J. Geophys. Res.*, *91*, 12,661–12,674, 1986.

McClusky, S. C., S. C. Bjornstad, B. H. Hager, R. W. King, B. J. Meade, M. M. Miller, F. C. Monastero, and B. J. Souter, Present day kinematics of the eastern California shear zone from a geodetically constrained block model, *Geophys. Res. Lett.*, *28*, 3369–3372, 2001.

Molnar, P., and P. Tapponnier, Cenozoic tectonics of Asia: Effects of a continental collision, *Science*, *189*, 419–426, 1975.

Northrup, C. J., L. H. Royden, and B. C. Burchfiel, Motion of the Pacific plate relative to Eurasia and its potential relation to Cenozoic extension along the eastern margin of Eurasia, *Geology*, *23*, 719–722, 1995.

Okada, Y., Surface deformation due to shear and tensile faults in a half-space, *Bull. Seismol. Soc. Am.*, *75*, 1135–1154, 1985.

Peltzer, G., P. Tapponnier, and R. Armijo, Magnitude of late Quaternary left-lateral displacements along the north edge of Tibet, *Science*, *246*, 1285–1289, 1989.

Roy, M., and L. H. Royden, Crustal rheology and faulting at strike-slip plate boundaries, 1. An analytic model, *J. Geophys. Res.*, *105*, 5583–5597, 2000.

Royden, L. H., B. C. Burchfiel, R. W. King, E. Wang, Z. Chen, F. Shen, and Y. Liu, Surface deformation and lower crustal flow in eastern Tibet, *Science*, *276*, 788–790, 1997.

Shen, Z. K., C. K. Zhao, A. Yin, Y. X. Li, D. D. Jackson, P. Fang, and D. N. Dong, Contemporary crustal deformation in east Asia constrained by Global Positioning System measurements, *J. Geophys. Res.*, *105*, 5721–5734, 2000.

Wang, Q., et al., Present-day crustal deformation in China constrained by Global Positioning System measurements, *Science*, *294*, 574–577, 2001.

Wu, J. C., Inverse analysis of crust deformation measurements, Ph.D. thesis, Hong Kong Polytech. Univ., Hong Kong, 1999.

Ye, H., B. T. Zhang, and F. Y. Mao, The Cenozoic tectonic evolution of the great north China: Two types of rifting and crustal necking in the great north China and their tectonic implications, *Tectonophysics*, *133*, 217–277, 1987.

Zeng, R. S., C. Y. Wang, and D. N. Zhang, On the dynamics of extensional basin, *Pure Appl. Geophys.*, *145*(3–4), 580–603, 1995.

Y. Q. Chen and H. W. Tang, Department of Land Surveying and Geo-Informatics, Hong Kong Polytechnic University, Hung Hom, Kowloon, Hong Kong, China. (lstang@polyu.edu.hk; lsyqchen@polyu.edu.hk)

Y. X. Li, First Crustal Deformation Monitoring Center, China Seismological Bureau, Tianjin, China 300180. (liyx@public.tpt.tj.cn)

J. C. Wu, Department of Surveying, Tongji University, Shanghai, China 200092. (jcwu@mail.tongji.edu.cn)